Conductive TiC/Ti–Cu/C composites fabricated by Ti–Cu alloy reactive infiltration into 3D-printed carbon performs

Carlos R Rambo[1], Nahum Travitzky[2] and Peter Greil[2]

Abstract

The microstructure and electrical properties of dense TiC/Ti–Cu/C composites fabricated by pressureless reactive infiltration of Ti–Cu alloy into porous starch-derived carbon preforms prepared by 3D printing was evaluated. Porosities in the range of 65–78 vol% were varied by post-isostatic pressing the as-printed preforms at pressures of 50–400 MPa. The reactive melt infiltration was carried out at 1100°C in a flowing Ar atmosphere and resulted in formation of a composite comprised predominantly of substoichiometric TiC, binary intermetallic Ti–Cu phases and residual carbon. Scanning electron microscopy analyses revealed a microstructure consisting of dispersed fine-grained TiC in a Ti–Cu matrix surrounded by a continuous carbon phase. Electrical resistivity measurements using the four-probe method were carried out and correlated to the composite microstructure. The electrical resistivity was evaluated in terms of carbon and TiC volume fractions.

Keywords

TiC/Ti–Cu/C composites, Ti–Cu alloy, 3D printing, reactive infiltration

Introduction

Ceramic particle-reinforced metal matrix composites (MMCs) are potential candidates for defence, automobile, aerospace, among several industrial applications. During the last decades, several processing routes were developed in order to decrease production costs and achieve adequate properties of advanced MMCs.[1–3] High temperature, hard MMCs with a wide range of compositions and controlled microstructure can be produced by compaction and forming of metal–ceramic powders.[4–6] Kaftelen et al.[4] produced Al–Cu matrix composites reinforced with TiC particulates by two distinct routes: mechanical alloying and flux-assisted casting of TiC and Al–4 wt.% Cu alloy mixtures. Powder processing approaches offer a variety of advantages; however, they are limited by slow and costly forming, consolidation and machining production steps. Alternatively, melt casting processes offer the possibility to produce dense composites with complex and near-net shapes in short time processing. On the other hand, melt casting of MMCs with fine and continuous ceramic phase is also an expensive and relatively complex route that demands high temperature processing (≥1200°C) or high infiltration pressures.[7]

The casting temperature and processing time can be substantially reduced by reactive infiltration processes, where the ceramic phase is then in situ formed through a simultaneous infiltration and reaction of a molten metal with the solid porous preform. Several processing routes based on in situ production of MMCs have been reported that resulted in the formation of a very fine, interpenetrating and thermodynamically stable reinforcing ceramic phase within an intermetallic matrix.[8–12] Al alloys (Al–Si, Al–Ti) and metallic Ti and Si are the most used for producing MMCs with carbide phases as

[1]Department of Electrical Engineering, Federal University of Santa Catarina, Florianópolis, Brazil
[2]Department of Materials Science, Glass and Ceramics, University of Erlangen-Nuernberg, Erlangen, Germany

Corresponding author:
Carlos R Rambo, Department of Electrical Engineering, Federal University of Santa Catarina, Florianópolis, Brazil.
Email: rambo@eel.ufsc.br

reinforcement by reactive melt infiltration into porous carbon performs.[13–15] Despite the advantages of molten metal casting techniques, the fabrication of MMCs with complex geometries is still a challenge. Rapid prototyping techniques emerged as one of the possible solutions to overcome such drawback, allowing the designing and manufacturing of complex-shaped composites at relatively low costs.[16]

3D printing of porous polymeric templates that can be pyrolyzed resulting in a porous carbon preform or even direct 3D printing of porous ceramic templates have attained great interest due to the possibility of realizing near-net shaped ceramics and composites by reactive molten metal infiltration.[17–19] Melcher et al.[19] fabricated dense Al_2O_3/Cu by Cu infiltration of porous Al_2O_3 produced by 3D printing.

Copper-based matrix composites are commonly employed in applications where a good electrical and/or thermal conductivity is required. Because of the high electrical conductivity of Cu, Cu-based matrix composites can be used as electrodes in electrical discharge machining (EDM).[20–23] In addition to the electrical conductivity, the electrode wear rate (EWR) and the material removal rate during machining are also key properties for composites intended to be used as electrodes in EDM.[21] As copper exhibits a relatively low melting temperature (1083°C), the losses during discharge are high and consequently its durability.[22] This durability, however, may be improved by the incorporation of a high melting point, electrically conductive and hard ceramic into the Cu matrix. Among ceramic candidates for this purpose, TiC is one of the most adequate candidate, characterized by a high hardness, very high melting point (3067°C) and low (metal-like) electrical resistivity (53–68 $\mu\Omega\cdot$cm).[24] Li et al.[25] reported that the EWR of TiC/Cu composites is lower than the wear rate of commercially available electrodes.

This work reports the production of TiC/Ti–Cu/C composites by pressureless low temperature reactive infiltration of a Ti–Cu alloy into porous carbon templates produced by 3D printing of starch. The microstructure and electrical properties of the final composites were evaluated.

Experimental

Commercially available starch–cellulose powder (ZP 14; Zcorporation, Burlington, USA) was used for the production of carbon preforms. After 3D printing of cellulose-starch bars (Zprinter 310, Zcorporation, Burlington, USA), the green preforms were submitted to isostatic pressing at pressures varying from 50 to 400 MPa. The performs were then pyrolyzed in N_2-atmosphere at 800°C for 1 h, in order to decompose the polymer into carbon. Porosities in the range of 65–78 vol% were achieved in the pyrolyzed samples. The density of the solid fraction (ρs) of the carbon preforms was measured by He-pycnometry (AccuPyc 1330, Micromeritics, USA). The percent porosity, ε, was estimated from the relation between the solid fraction density and the geometrical density (ρ_G), according to the expression: $\varepsilon = (1 - \rho_G/\rho s) \times 100$.

The as-fabricated porous carbon preforms with dimensions of $15 \times 10 \times 5$ mm were used for post-reactive melt infiltration with a Ti–Cu alloy (50 wt%Ti–50 wt.%Cu; Hauner Metallische Werkstoffe, Germany). A 30-min exposure at 1100°C in Ar atmosphere ensured spontaneous reactive infiltration of the carbon preform with the Ti–Cu alloy driven by capillarity force. Details of the infiltration procedure are shown in previous publication.[14]

The phase evaluation of the samples was conducted by X-ray diffractometry (XRD) using Cu-Kα radiation. Samples were scanned in a powder diffractometer (D 500; Siemens, Karlsruhe/Germany). Scanning electron microscopy (SEM, Quanta 200; FEI, Czech Republic) coupled with energy dispersive spectroscopy (EDS, Inca x-sight; Oxford Instruments, UK) were applied for microstructure and elemental characterization. The volume fraction of the phases was obtained by stereological analysis of the SEM micrographs (ImageJ). For each sample, a set of six pictures was recorded and the mean phase fraction was statistically estimated. The electrical resistivity of the composites was measured by a micro-ohmemeter (T5R2, AOIP; Ris Orangis, France) using the four-point probe method at room temperature. Several measurements were conducted in order to exclude the effect of contact resistance. The extremities of the samples were covered by a thin silver film, which improved the contact between the sample and the electrodes.
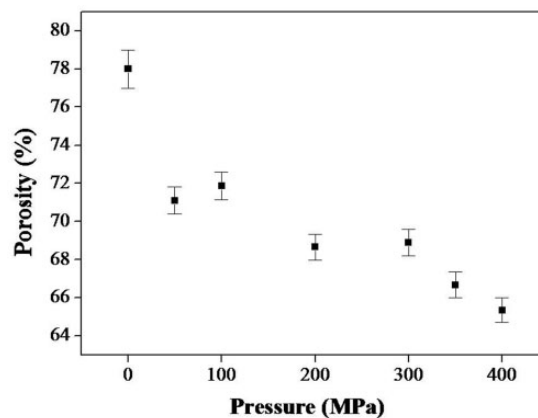
Figure 1. Porosity of the pyrolyzed performs versus post-isostatic pressure of the green performs.

Results and discussion

Figure 1 shows the porosity of the pyrolyzed performs versus function of the isostatic pressure of the green preforms. By a maximal pressure of 400 MPa, a porosity of 65 vol% was achieved.

After 3D printing and pyrolysis, a homogeneous structure with skeleton density of $1.8 \pm 0.1 \, g/cm^3$ and pore size ranging from 50 to 100 μm, which provides an open path for infiltration, were obtained for all samples with different porosities. A continuous network of carbon struts with thickness varying between a few μm up to 100 μm provided the necessary mechanical

Table 1. Phase composition (mean values) of the final composites based on image analysis.

Carbon (%)	TiC (%)	Ti–Cu alloy (%)
47.0 ± 0.2	19.7 ± 0.6	33.3 ± 0.6
45.8 ± 0.5	21.3 ± 0.5	32.9 ± 0.6
43.6 ± 0.5	24.7 ± 0.5	31.7 ± 0.6
41.9 ± 0.5	23.1 ± 0.7	34.9 ± 0.5
39.7 ± 0.4	24.3 ± 0.5	36.0 ± 0.4
37.2 ± 0.4	18.1 ± 0.6	44.7 ± 0.5
23.0 ± 0.2	44.2 ± 0.6	32.8 ± 0.3
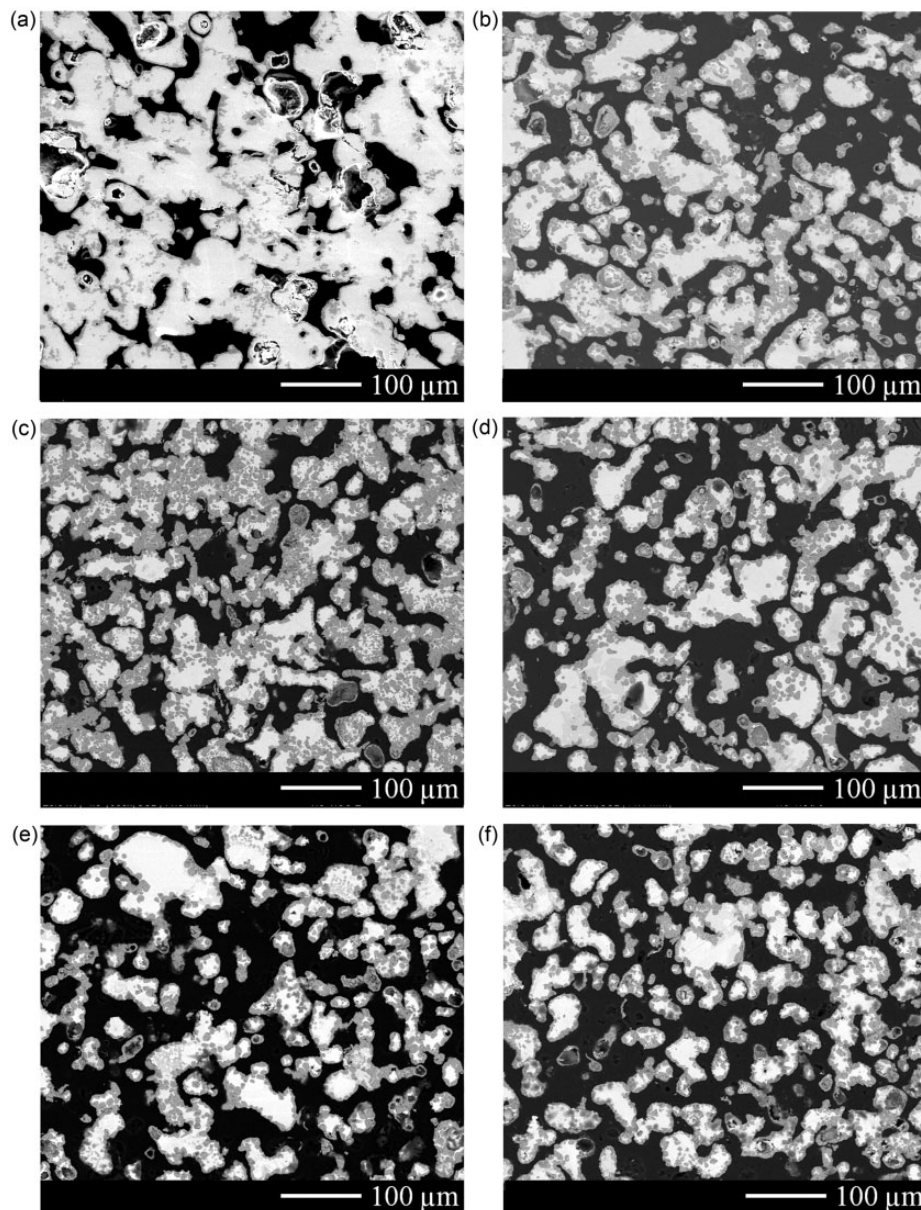
Figure 2. SEM micrographs of polished cross sections of the TiC/Ti–Cu/C composites produced by infiltration into C performs with different mean porosities: (a) 78.0; (b) 71.8; (c) 71.1; (d) 68.9; (e) 66.7; and (f) 65.3.

stability for handling. A nearly complete reactive infiltration of carbon preforms with Ti–Cu alloy was obtained after 30 min at 1100°C. According to XRD analysis, the composites comprised cubic (JCPDS 73-0472) TiC and tetragonal Cu_4Ti_3 (JCPDS 18-0460) as two major crystalline phases.

Table 1 shows the phase composition of the final composites in function of decreasing carbon phase content. As the carbon fraction decreases, the amount of TiC formed increases as expected. The metallic fraction remains in the range of 15–25%, varying according to the availability of Ti in the matrix.

The composition of the matrix at the Ti–Cu/C interface varies according to the Ti consumed for the TiC forming reaction, which depends on the kinetics of reaction and diffusion rates of the constituents. This issue will be not discussed here as the samples were prepared under only one time and temperature condition.

Figure 2 shows SEM micrographs of the final composites. The representative microstructures of samples with initial porosity varying from 78% (Figure 2(a)) to 65% (Figure 2(f)) revealed distinguished features. The bright phase is the Ti–Cu matrix, the grey phase represents the TiC and the dark/black phase is the non-reacted carbon.

In Figure 2(a) and (b), the metal matrix (grey phase) appears as major phase in the microstructure, while in Figure 2(c) and (d), TiC (dark grey phase) is seen as predominant non-carbon phase. In the sample with the lowest porosity (Figure 2(a)) more carbon reacted into TiC than in the sample with higher porosity (Figure 2(f)). All samples exhibit also very low final porosity, with exception of the sample with higher matrix content after infiltration reaction. All samples exhibit homogenous TiC grain distribution surrounding the matrix phase, within a continuous carbon network. TiC grains grew up from the interface reaction between Ti form the Ti–Cu alloy and carbon. The observed size of the TiC grains is in the range of 5 to 10 μm for all samples. The reaction for Ti formation and subsequent grain growth occurs through carbon diffusion into the TiC phase, towards the Ti–Cu matrix, rather than Ti diffusion into carbon, since the diffusivity of carbon in TiC is known to be very high.[26] Moreover, although carbon diffuses through TiC consuming Ti from the matrix, dissolution of Ti in the matrix may also occur.[27] All TiC grains are completely surrounded by the metal phase (Figure 2(e)), revealing the good wettability of Cu on TiC, as already observed by Sabatello et al.[28] As the initial porosity decreased (from Figure 2(a) to (f)), the fraction of carbide and matrix phases and the continuity of these phases decreased, which would contribute for the decreasing in the electrical conductivity.

Figure 3 shows the electrical resistivity in function of the fraction of remaining carbon in the composites. As expected, the resistivity increases with the carbon content in the composites.

Several models were developed to evaluate the electrical resistivity of bi-phasic MMCs.[29,30] Chang et al.[31] reported that the resistivity of the composite depends on the distribution and geometry of the reinforcement in the matrix. The electrical resistivity of metal matrix composites, in which the reinforcement is also an electric conductor, increases with increasing the volume fraction of the component with higher resistivity. To better evaluate the role of the resistive phases (TiC and C) and Ti–Cu matrix, the electrical resistivity of the composites was evaluated in terms of the relative volume fraction of TiC (Φ_{TiC}) in the bi-phase component TiC/C as the resistive part of the composite

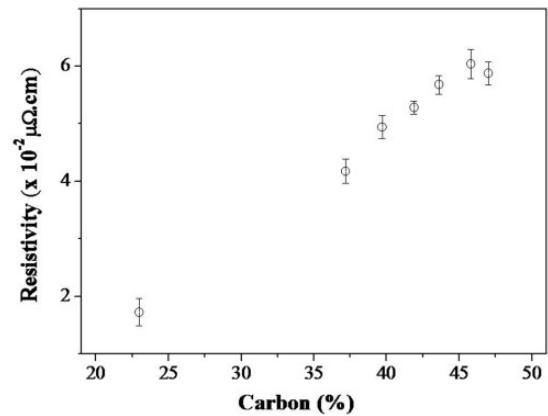$$\Phi_{TiC} = \frac{V_{TiC}}{V_{TiC} + V_C} \qquad (1)$$

Figure 3. Electrical resistivity of the TiC/Ti–Cu/C composite versus relative volume fraction of C.
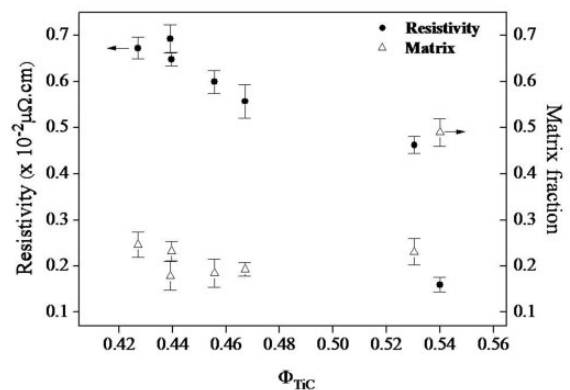
Figure 4. Electrical resistivity and matrix volume fraction of the TiC/Ti–Cu/C composite versus relative volume fraction of TiC.

Figure 4 shows the electrical resistivity and the matrix volume fraction in function of the relative TiC volume fraction (Φ_{TiC}) in the composite.

The resistivity of the composite decreases with increasing relative TiC fraction, while the matrix fraction remains in the range of 15–25% as shown before. A very low resistivity was measured for the composite with a relative TiC volume fraction of 0.54 (16 $\mu\Omega\cdot$cm). It can be assumed that the higher volume fraction of the matrix (0.50) contributed to the resistivity drop. The sample with an initial perform porosity of 65% exhibits the highest resistivity (60 $\mu\Omega\cdot$cm). The lower resistivity was measured for samples with higher matrix volume fraction. On the other hand, for the sample with the second lowest resistivity (42 $\mu\Omega\cdot$cm), the resistivity seems to be more affected from the TiC fraction ($V_{TiC} = 0.37$), than directly from the matrix.

Conclusions

Conductive TiC/Ti–Cu/C composites were synthesized by Ti–Cu alloy reactive melt infiltration into porous carbon preformed by 3D printing. The material consisted of TiC, Ti–Cu phases and residual C. Control over the volume fraction of initial porosity in the carbon preform may lead to denser TiC-reinforced composites. The low electrical resistivity (15–60 $\mu\Omega\cdot$cm) of the samples makes the new TiC/Ti–Cu/C composites a very promising candidate for electrical–mechanical applications. Using a low-melting metal alloy with the ability of the porous carbon preforms to be machined by 3D printing in a large variety of geometries may attain the interest for new processing technologies with a wide range of technological applications, including EDM electrodes. Low-cost and rapid manufacturing of ceramic-reinforced MMCs with high electrical conductivity opens a wide range of possibilities, leading to the design of new complex-shaped tools.

Conflict of interest

None declared.

References

1. Travitzky N, Kumar P, Sandhage KH, et al. Rapid synthesis of Al_2O_3 reinforced Fe-Cr-Ni composites. *Mater Sci Eng A* 2003; 344: 245–252.
2. Vasić S, Grobéty B, Kuebler J, et al. Activation mechanism and infiltration kinetic for pressureless melt infiltration of Ti activated Al_2O_3 preforms by high melting alloy. *Adv Eng Mater* 2009; 11: 659–666.
3. Manna A, Bains HS and Mahapatra PB. Experimental study on fabrication of Al-Al_2O_3/Grp metal matrix composites. *J Compos Mater* 2011; 45: 2003–2010.
4. Kaftelen H, Ünlü N, Göller G, et al. Comparative processing-structure-property studies of Al–Cu matrix composites reinforced with TiC particulates. *Compos Part A Appl Sci* 2011; 42: 812–824.
5. Stoloff NS. *Metals handbook*. Vol. 1, 10th ed. Metals Park, OH: ASM International, 1990, p.951.
6. Jenei P, Gubicza J, Yoon EY, et al. High temperature thermal stability of pure copper and copper–carbon nanotube composites consolidated by high pressure torsion. *Compos Part A Appl Sci* 2013; 51: 71–79.
7. Asthana R. Cast metal–matrix composites. II: process fundamentals. *J Mater Synth Process* 1997; 5: 339.
8. Weber S and Theisen W. Sintering of high wear resistant metal matrix composites. *Adv Eng Mater* 2007; 9: 165–170.
9. Fahrenholtz WG, Ewsuk KG and Loehman RE. Kinetics of ceramic-metal composite formation by reactive metal penetration. *J Am Ceram Soc* 1998; 81: 2533–2541.
10. Travitzky N, Gotman I and Claussen N. Alumina-Ti aluminide interpenetrating composites: microstructure and mechanical properties. *Mater Lett* 2003; 57: 3422–3426.
11. Wagner F, Garcia DE, Krupp A, et al. Interpenetrating Al_2O_3-$TiAl_3$ alloys produced by reactive infiltration. *J Eur Ceram Soc* 1999; 19: 2449–2453.
12. Claussen N. Processing of advanced ceramic composites: issues of producibility, affordability, reliability, and tailorability. *Br Ceram Trans* 1999; 98: 256–257.
13. Lyckfeldt O and Ferreira JMF. Processing of porous ceramics by starch consolidation. *J Eur Ceram Soc* 1998; 18: 131–140.
14. Rambo CR, Travitzky N, Zimmermann K, et al. Synthesis of TiC/Ti–Cu composites by pressureless reactive infiltration of TiCu alloy into carbon preforms fabricated by 3D-printing. *Mater Lett* 2005; 59: 1028–1031.
15. Greil P. Near net shape manufacturing of ceramic. *Mater Chem Phys* 1999; 61: 64–68.
16. Kumar S and Kruth J-P. Composites by rapid prototyping technology. *Mater Design* 2010; 31: 850–856.
17. Zhang W, Travitzky N and Greil P. Formation of $NbAl_3$/Al_2O_3 composites by pressureless reactive infiltration. *J Am Ceram Soc* 2008; 9: 3117–3120.
18. Yin X, Travitzky N and Greil P. Near-net-shape fabrication of Ti_3AlC_2-based composites. *Int J Appl Ceram Technol* 2007; 4: 184–190.
19. Melcher R, Martins S, Travitzky N, et al. Fabrication of Al_2O_3-based composites by indirect 3D-printing. *Mater Lett* 2006; 60: 572–575.
20. Li L, Wong YS, Fuh JYH, et al. Effect of TiC in copper–tungsten electrodes on EDM performance. *J Mater Process Technol* 2001; 113: 563–567.
21. Tsai HC, Yan BH and Huang FY. EDM performance of Cr/Cu-based composite electrodes. *Int J Mach Tools Manuf* 2003; 43: 245–252.

22. Zaw HM, Fuh JYH, Nee AYC, et al. Formation of a new EDM electrode material using sintering techniques. *J Mater Process Technol* 1999; 89–90: 182–186.

23. Norasetthekul S, Eubank PT, Bradley WL, et al. Use of zirconium diboride-copper as an electrode in plasma applications. *J Mater Sci* 1999; 34: 1261–1270.

24. Pierson HO. *Handbook of refractory carbides and nitrides*. Westwood, New Jersey, USA: Noyes Publications, 1996.

25. Li L, Wong YS, Fuh JYH, et al. EDM performance of TiC/copper-based sintered electrodes. *Mater Des* 2001; 22: 669–678.

26. Dahan I, Admon U, Frage N, et al. Diffusion in Ti/TiC multilayer coatings. *Thin Solid Films* 2000; 377–378: 687–693.

27. Suzuki S, Hirabayashi K, Shibata H, et al. Electrical and thermal conductivities in quenched and aged high-purity Cu–Ti alloys. *Scripta Mater* 2003; 48: 431–435.

28. Sabatello S, Frage N and Dariel MP. Graded TiC-based cermets. *Mater Sci Eng A* 2000; 288: 12–18.

29. Lilly AC, Deevi SC and Gibbs ZP. Electrical properties of iron aluminides. *Mater Sci Eng A* 1998; 258: 42–49.

30. Aldrich DE, Fan Z and Mummery P. Processing, microstructure and physical properties of interpenetrating Al_2O_3/Ni composites. *Mater Sci Technol* 2000; 16: 747–752.

31. Chang S-Y, Chen C-F, Lin S-J, et al. Electrical resistivity of metal matrix composites. *Acta Mater* 2003; 51: 6191–6302.